

Fuzzy-PI Controller Design for PM Wind Generator to Improve Fault Ride Through of Wind Farm

Marwan Rosyadi^{*‡}, S. M. Muyeen^{**}, Rion Takahashi^{*}, Junji Tamura^{*}

^{*}Department of Electrical and Electronic Engineering, Kitami Institute of Technology

^{**}Department of Electrical Engineering, the Petroleum Institute

marwanrosyadi@yahoo.co.id, smmuyeen@pi.ac.ae, rtaka@mail.kitami-it.ac.jp, tamuraj@mail.kitami-it.ac.jp

[‡]Corresponding Author; Marwan Rosyadi, 165 Koen-cho Kitami-Hokkaido Japan, +81 157-26-9273, marwanrosyadi@yahoo.co.id

Received: 03.02.2013 Accepted: 24.03.2013

Abstract- This paper presents an application of Fuzzy-PI controller to current controller of voltage source converter based permanent magnet wind generator in order to improve Fault Ride through (FRT) capability of wind farm. Fuzzy logic controller is proposed to adjust PI controller gain parameters. Fuzzy rule base and the inference mechanism of the fuzzy logic controller (FLC) are designed based on gain and phase margin analysis plotted on the bode diagram characteristic. To evaluate the controller system capabilities, simulation analyses are performed on a model system composed of two wind farms connected to an infinite bus. Simulation results by PSCAD/EMTDC show that the proposed controller is very robust and effective to improve the FRT of wind farm during fault in the grid system.

Keywords- Fuzzy Logic Control, PMSG, voltage source converter, fault ride through, wind farm.

1. Introduction

Due to the increasing concerns about decreasing pollution production and improving environmental conditions, recently the integration of large scale wind farms into electrical network system have been significantly increased. Global Wind Energy Council (GWEC) predicted that global wind power generation capacity will reach to 459 GW and new capacity of 62.5 GW will be added to the global total at the end of 2015 [1]. It is well known that power production of wind generator fluctuates depending on wind speed variations which affects power system stability and power quality [2]-[5]. Increasing of the penetration level of the wind generator into grid system has led power system operators to revise the grid code connection requirements for their power system in many countries [6]. The grid code prosecutes that the wind generator should give a contribution to control the power in case of abnormal operating conditions such as network disturbance. The low voltage ride through grid code requirement should be taken into account for a short circuit fault in grid system. Out of synchronism of a large number of wind generators can have serious impact on power system stability. Therefore, the interaction between

wind farm and power system has become important to be analyzed in the few last years.

The Fixed Speed Wind Turbines with Induction Generator (FSWT-IG) is the simplest type compared with others and is most widely installed in wind farms [7]. However, the main problem of FSWT-IG is that it does not have any fault ride trough capability for a voltage dip in the grid system [8]-[10]. During fault in the grid system, the induction wind generators require large reactive power to recover the air gap flux [9]. If sufficient reactive power is not supplied, the induction generator becomes unstable and it requires to be disconnected from the grid system. Utilization of Flexible AC Transmission Systems (FACTS) devices has become the better choice due to their advantages of good damping performance for power system dynamic oscillations [11]-[14]. However, the system overall cost will be expensive when FACTS devices are installed at a FSWT-IG based wind farm.

Variable Speed Wind Turbine with Permanent Magnet Synchronous Generator (VSWT-PMSG) is attractive type of wind turbine technology. The VSWT-PMSG system is equipped with AC/DC/AC electronic converters in which the

active and reactive power produced by PMSG can be controlled. Accordingly, the wind generator has strong low voltage ride through capability [15]-[17]. However, this type of wind generator is expensive compared with other types. Therefore, combined installation of VSWT-PMSG and FSWT-IG in a wind farm can be efficient due to reduced system investment cost.

Conventional PI controller is very common in the control of the AC/DC/AC converter of PMSG due to their simple structure and good performances in a wide range of operating conditions. The PI controllers are simple but cannot always effectively control systems with changing parameters or strong nonlinearities. Change of parameters in the grid system, especially in a fault condition, leads significant impact on the control system performance of the converter. The deviation of the grid system impedance will change gain margin and phase margin of the control system. Therefore, the PI controller should have a function of online retuning of their parameters.

On the other hand, fuzzy logic controller has attracted the attention of researchers because it can deal with nonlinear systems and does not need precise mathematical modelling of the system [18]. Compared with conventional PI controller, fuzzy logic controller has the potential to provide an improved performance even for a system with wide parameter variations [19]. The fuzzy logic controller has advantages of robust, simple, easily to be modified, usable for multi input and output sources, and to be implemented very quickly and cheaply. Integration of fuzzy logic control with conventional PI controller (Fuzzy-PI controller) can be an effective way to solve the problem of system parameter change. The fuzzy logic control can be used to adjust the gain parameters of PI controller for any operating conditions. Hence, a good control performance can be achieved. Therefore, application of Fuzzy-PI controller on the PMSG converter controller system is proposed in this paper.

2. Power System Model

The power system model used in this study is shown in Fig. 1. Wind Farm 1 (WF 1) with VSWT direct drive PMSG rated at 5 MW is connected to the infinite bus through a back to back (AC/DC/AC) power converter, a filter inductance, a 1.0/66 kV step up transformer and a double circuit transmission line. The rated frequency of the PMSG is 20 Hz. WF 2 with FSWT-IG rated at 10 MW is also connected to the infinite bus via a 0.69/66 kV step up transformer and a single circuit transmission and double circuit transmission lines. WF 1 and WF 2 are connected at point of common connection (PCC). In order to compensate reactive power consumption by IG, a capacitor bank (Qc) is installed in Wind Farm 2. The value of the capacitor is determined so that the power factor becomes unity at rated power operation. The resistance and reactance of the transmission line are represented in the form of R+jX as shown in the figure, respectively. Parameters of PMSG and IG are shown in Table I. The system base is 10 MVA and grid frequency is 50 Hz.

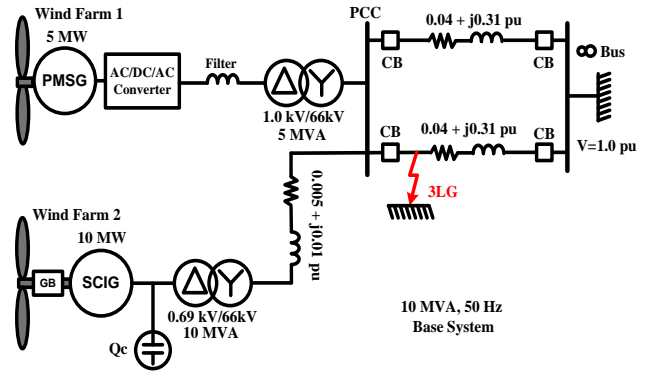


Fig. 1. Model System

Table 1. Generators parameter

	Rated	5 MW		Rated	10 MW
	PMSG	R_s		0.01 pu	IG
	L_s	0.06 pu		L_s	0.046 pu
	X_d	0.9 pu		L_m	3.86 pu
	X_q	0.7 pu		Rr_1	0.298 pu
	ψ_m	1.4 pu		Rr_2	0.018 pu
	H	3.0 s		Lr_1	0.122 pu
				Lr_2	0.105 pu
				H	3.0 s

3. Wind Turbine Model

The mechanical power output of wind turbine captured from the wind power can be calculated as follows [20]:

$$P_w = 0.5\rho\pi R^2 V_w^3 C_p(\lambda, \beta) \tag{1}$$

where P_w is the captured wind power (W), ρ is the air density (Kg/m³), R is the radius of rotor blade (m), V_w is wind speed (m/s), and C_p is the power coefficient.

The value of C_p is dependent on tip speed ratio (λ) and blade pitch angle (β) based on the turbine characteristics as follows [20]:

$$C_p(\lambda, \beta) = c_1 \left(\frac{c_2}{\lambda_i} - c_3\beta - c_4 \right) e^{-\frac{c_5}{\lambda_i}} + c_6\lambda \tag{2}$$

with

$$\frac{1}{\lambda_i} = \frac{1}{\lambda - 0.08\beta} - \frac{0.035}{\beta^3 + 1} \tag{3}$$

where c_1 to c_6 denote characteristic coefficients of wind turbine ($c_1=0.5176$, $c_2=116$, $c_3=0.4$, $c_4=5$, $c_5=21$ and $c_6=0.0068$).

The C_p - λ performance characteristic of wind turbine is shown in Fig. 2. The optimum value of power coefficient ($C_{p_{opt}}$) is 0.48 at $\lambda = 8.1$ with $\beta = 0^0$. This value of λ is set as the optimal value (λ_{opt}). Fig. 3 depicts the characteristic between the turbine power output and the rotor speed for different wind speeds. The maximum power output (1 pu) of

wind turbine is obtained at 12 m/sec wind speed and 1 pu rotational speed.

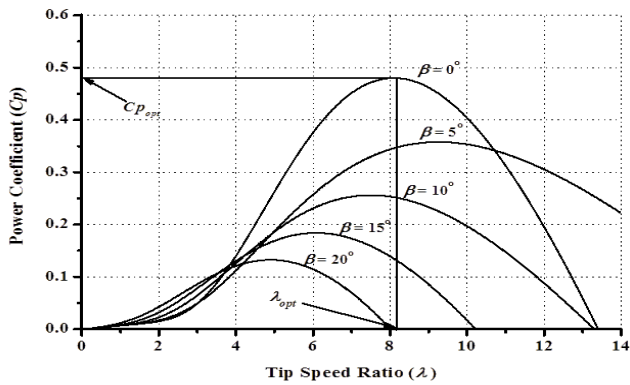


Fig. 2. Cp - λ characteristic of wind turbine

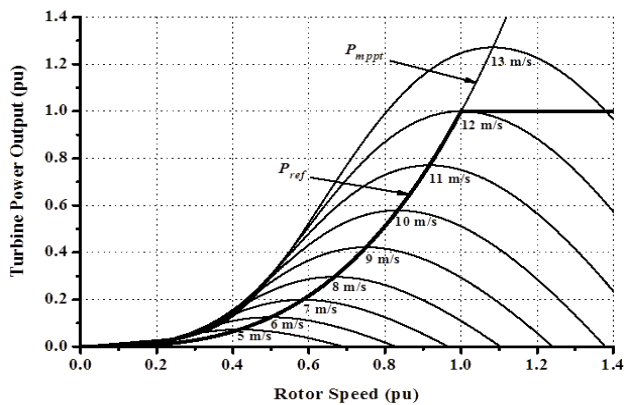


Fig. 3. Turbine power characteristic (β = 00)

In variable speed wind turbine system, the rotor speed of wind turbine (ω_r) is measured in order to determine the Maximum Power Point Tracking (MPPT). The maximum power (P_{mppt}) is calculated without measuring the wind speed as expressed in eq. (4) [17]. The reference power (P_{ref}) is limited within the rated power of generator.

$$P_{mppt} = 0.5 \rho \pi R^2 \left(\frac{\omega_r R}{\lambda_{opt}} \right)^3 C_{p_{opt}} \quad (4)$$

4. PMSG Control System

Detail of proposed control system for VSWT-PMSG is shown in Fig. 4. The VSWT-PMSG consists of the following components: a direct drive PMSG, back to back converters based on two levels of IGBT which are composed of stator side converter (SSC) and grid side converter (GSC), a DC-link circuit composed of a chopper with a resistance (R_c) and a capacitor (C_{dc}), two voltage source converter controllers (stator side controller and grid side controller), L filter, and step up transformer.

The SSC is connected to the stator of PMSG, and it converts the three phase AC voltage generated by PMSG to DC voltage. The three phase voltage and current are detected on the stator terminal of PMSG. The rotor speed of PMSG is obtained from the rotor of the generator. All outputs of the sensors are fed to the stator side controller as input signals in order to control the voltage references of the stator side voltage source converter for modulation.

The stator side controller scheme is shown in Fig. 5. The aim of the stator side controller is to control active and reactive power output of the PMSG. The current control loop is designed based on the d-q rotating reference frame. The rotor angle position (θ_r) used in the transformation between abc and dq variables is obtained from the rotor speed of generator. The active power (P_s) and reactive power (Q_s) of the generator are controlled by the d-axis current (I_{sd}) and the q-axis current (I_{sq}), respectively. The value of active power reference (P_{ref}) is determined by MPPT method of the wind turbine characteristic as shown in Fig. 3. The reactive power reference (Q_s^*) is set to zero for unity power factor operation. The cross couplings $I_{sd}\omega_e L_s$ and $I_{sq}\omega_e L_s$ should be compensated at the output of the current controllers in order to improve tracking capability of the control system. Finally, V_{sd}^* and V_{sq}^* are voltage reference of current controller which is used to generate the three phase reference voltage (V_{sa}^* , V_{sb}^* , V_{sc}^*) to control stator currents of the PMSG.

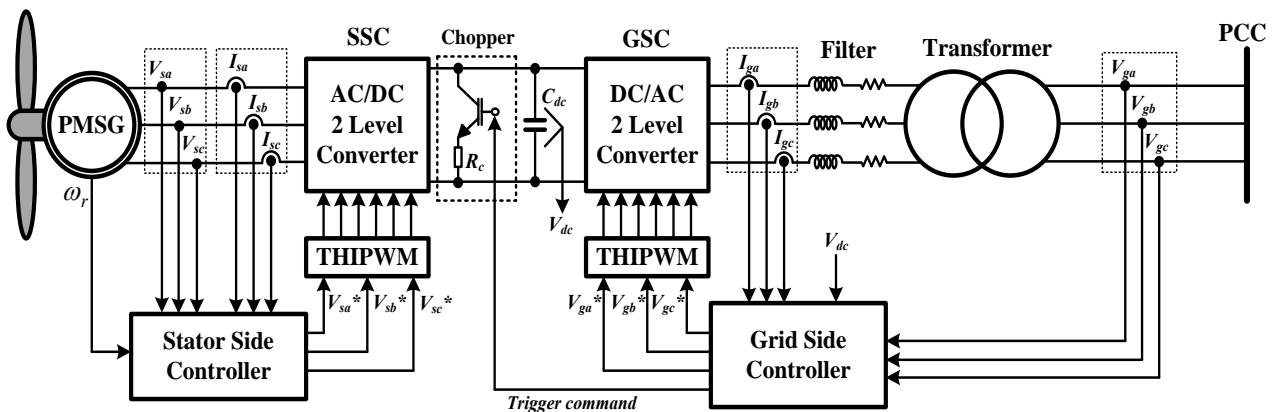


Fig. 4. PMSG control system

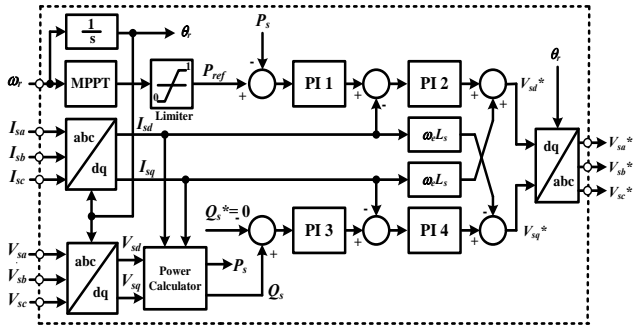


Fig. 5. Stator side controller

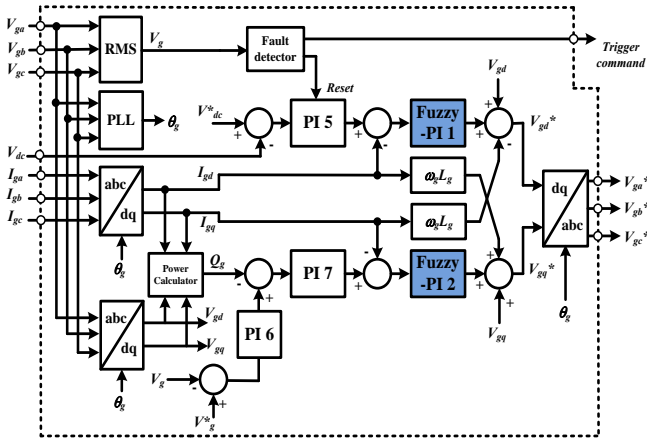


Fig. 6. Grid side controller

The GSC converts DC voltage into three phase AC voltage of the grid frequency. The converter is connected to the grid system through L filter and a step up transformer. The grid current and voltage are detected on the output of GSC and the high voltage side of the transformer, respectively. The DC voltage (V_{dc}) is detected on the DC capacitor.

Fig. 6 shows a block diagram of the grid side controller system. In this control strategy, the control system based on the d-q rotating reference frame is implemented which has same rotational speed as the grid voltage. The three phase grid currents (I_{ga} , I_{gb} , I_{gc}) and the grid voltages (V_{ga} , V_{gb} , V_{gc}) are transferred into the d-q rotating reference frame by using Park transformation. The Phase Locked Loop (PLL) is used to extract the grid side phase angle (θ_g). The controller is divided into two cascade loop control, one for active power and the other is for the reactive power. When grid voltages on the stationary reference frame are transformed into the d-q rotating reference frame, V_{gd} is set to constant and V_{gq} is set to zero. Therefore, the active and reactive power delivered to the grid can be controlled separately by the d-axis current (I_{gd}) and the q-axis current (I_{gq}), respectively. The voltage of DC-link capacitor (V_{dc}) is maintained constant in order to transfer the active power generated by PMSG to the grid. The d-axis current reference signal (I_{gd}^*) is determined from output of the DC-voltage controller, and the q-axis current reference signal (I_{gq}^*) is obtained so that the grid terminal voltage (V_g) is kept constant at 1 pu. In order to improve tracking capability of control system, the cross coupling should be canceled by adding $I_{gd}\omega L_g$ and $I_{gq}\omega L_g$ at the output

of the current controllers. The output of current controller (V_{gd}^* and V_{gq}^*) is transformed into the stationary reference frame (V_{ga}^* , V_{gb}^* , V_{gc}^*) which is used as reference signal for pulse wave modulation. In fault condition, the active power transferred to the grid is set to zero by resetting PI5 in order to maximize the reactive power support and at the same time the fault detector sends the *trigger command* for activation of the DC link protection. The fault detector is activated when the grid voltage decreases under 0.95 pu.

The grid side converter has important role to ensure the active and reactive power delivered to the network effectively. Change of parameters in the grid system leads significant impact on the control system performance of the converter especially in fault condition. The deviation of the grid system impedance will change gain margin and phase margin of the control system. Because the GSC is directly connected to the grid system, to control the dq-axis current loop in the grid side controller the Fuzzy-PI controller is proposed. The control strategy for the Fuzzy-PI controller will be explained in Section V.

In modulation technique, Third Harmonic Injection Pulse Wave Modulation (THIPWM) is used in this work. Injection of third harmonic in the reference voltage makes it possible to utilize the voltage reference without over modulation. In addition, the THIPWM can maximize fundamental amplitude of the output voltage [21].

5. Fuzzy-PI Controller Design

In this study, the d-axis and the q-axis components are assumed identical, and hence the current loop control system can be analyzed by using one axis component only. Block diagram of Fuzzy-PI controller for d-axis current component is shown in Fig. 7. Here FLC adjust the PI parameters according to operating conditions, e.g., the error (e) and change in error (de) of the input signals, which characterizes its first time derivative during process control. To determine control signal for proportional gain (K_p), inference engine with rule base having if-then rules in the form of “If e and de , then K_p ” is used.

Figs. 8 and 9 show the membership function for input e/de and output K_p . The variables fuzzy subsets for input e/de are Negative Big (NB), Negative Small (NS), Zero (Z), Positive Small (PS), and Positive Big (PB). Due to the variation of the d-axis or q-axis current between -1 to 1 pu, the range of input membership function is also set at this interval. The variables fuzzy subsets for output K_p are Small (SM), Medium (MD) and Big (BG). Table 2 shows fuzzy control rule base for gain K_p . In this work, Mamdani’s max-min method is used for inference mechanism. The center of gravity method is used for defuzzification.

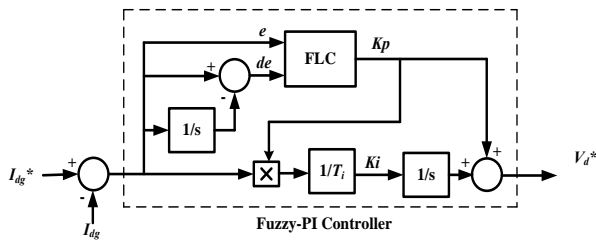


Fig. 7. Fuzzy-PI controller

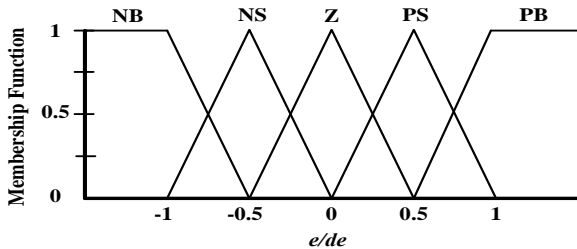


Fig. 8. The membership function for input e/de

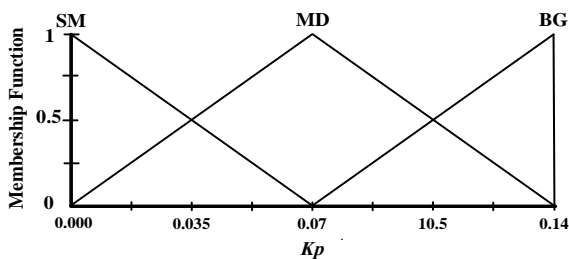


Fig. 9. The membership function for output Kp

Table 2. Fuzzy control rule base

e/de	NB	NS	Z	PS	PB
NB	BG	BG	MD	BG	BG
NS	BG	MD	SM	MD	BG
Z	MD	SM	SM	SM	MD
PS	BG	MD	SM	MD	BG
PB	BG	BG	MD	BG	BG

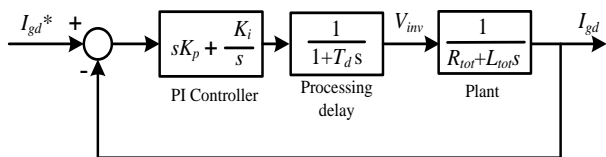


Fig. 10. The d-axis current loop control of GSC

In order to design the membership function for output of K_p , block diagram of current loop control shown in Fig. 10 is used for dynamic stability analysis. The controller is composed of a PI controller, a processing delay, and a plant system. The time delay (T_d) is composed of one sample delay caused by switching frequency ($T_s=1/f_s$) and one half sample delay caused by the dead time of PWM converter ($T_{cnv}=1/2T_s$). The transfer function (I_{gd}/V_{inv}) can be expressed as $1/(R_{tot} + L_{tot}s)$, where I_{gd} is current output on grid side of transformer, V_{inv} is voltage output of converter, L_{tot} and R_{tot} are total inductance and resistance of L filter and transformer, respectively. The integral time constant (T_i) of PI controller is set equal to the plant system time constant

(L_{tot}/R_{tot}). Proportional gain K_p can be selected by analyzing the frequency response of the bode diagram with 3 kHz switching frequency of GSC selected. Finally, the integral gain value can be obtained by $K_i = K_p/T_i$.

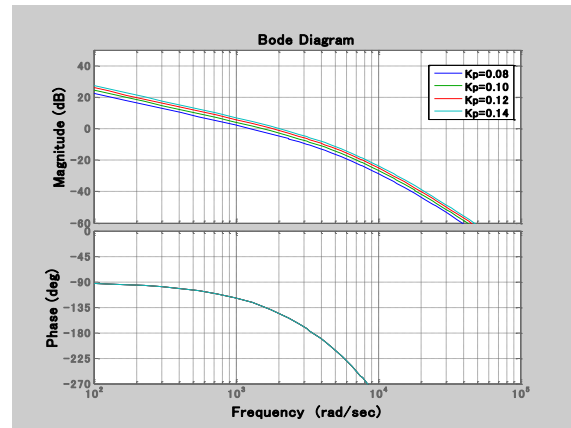


Fig. 11. Bode diagram of the current loop control of GSC

Fig. 11 shows a bode diagram of the current loop control of GSC for four different gain K_p . In this study, in order to stabilize the current loop, gain margin (Gm) larger than 6 dB and phase margin (Pm) larger than 45 deg are required. The bode diagram shows that maximum gain K_p of 0.14 is obtained. Therefore, the range of membership function for output K_p is set at [0.0 to 0.14] as shown in Fig. 9.

6. Simulation Results

A symmetrical three-line-to-ground (3LG) fault at the transmission line as shown in Fig. 1 is considered as network disturbance. The fault occurs at 0.1 sec, the circuit breakers (CB) on the faulted line are opened at 0.2 sec, and at 1.0 sec the CBs are re-closed. The wind speeds for the wind generators are kept constant at the rated speed. Two cases are investigated in the simulation study to show the effective-ness of the proposed control strategy. First, simulation study is performed in which the Fuzzy-PI controller is applied to GSC of PMSG. Second, simulation study is performed using the model system in which the conventional PI controller is applied. Simulations were performed by using PSCAD/ EMTDC.

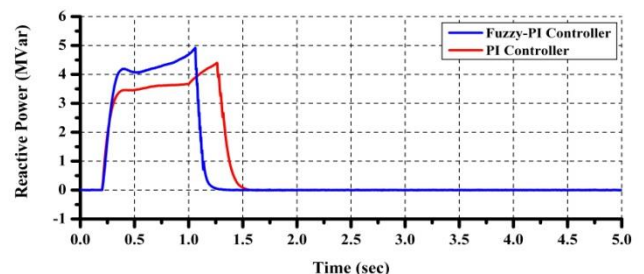


Fig. 12. Reactive power output of PMSG

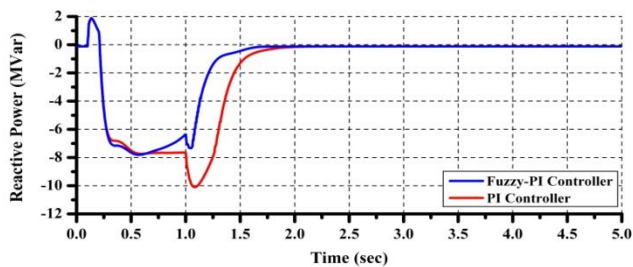


Fig. 13. Reactive power output of IG

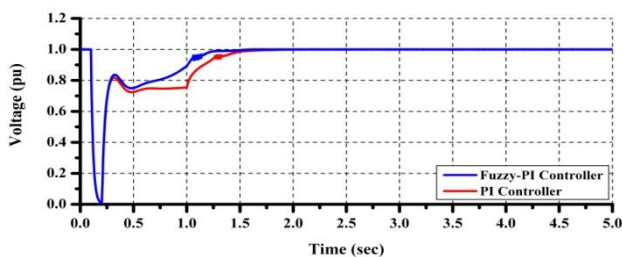


Fig. 14. Terminal voltage at PCC

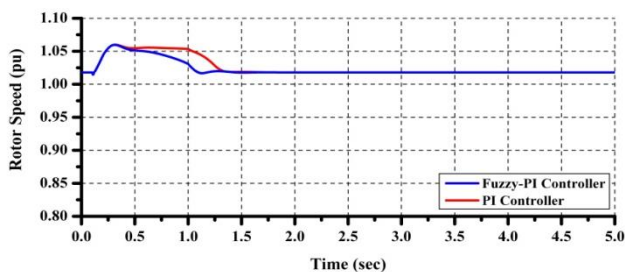


Fig. 15. Rotor speed response of IG

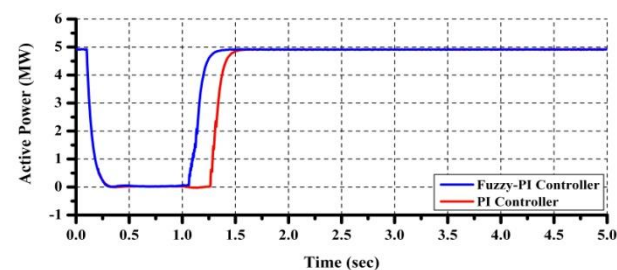


Fig. 16. Active power output of PMSG

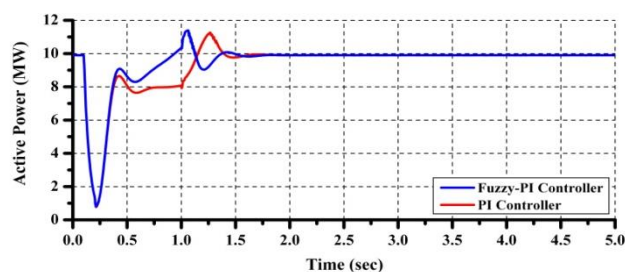


Fig. 17. Active power output of IG

Figs. 12 and 13 show responses of reactive powers, from which it is seen that the grid side converter of WF 1 can provide necessary reactive power during the symmetrical 3LG fault. Therefore terminal voltage of the wind farms at PCC can return back to the rated value quickly as shown in Fig. 14. The rotor speed of IG in WF 2 is also return back

to initial condition as shown in Fig. 15. Figs. 16 and 17 show responses of the active power output of PMSG and IG, respectively. From Figs. 12 through 17, it can be seen that the performances of the wind farms can be stabilized more effectively in the case of VSWT-PMSG with the Fuzzy-PI controller than that with conventional PI controller.

7. Conclusion

In this paper Fuzzy-PI controller is proposed in the grid side converter controllers of Variable Speed Permanent Magnet Wind Generator (PMSG) to improve its fault ride through capability as well as the performance of the neighboring wind farm composed of Fixed Speed Wind Generators. The controller combines fuzzy logic to classical PI controller to adjust online the PI gains. The results show that the proposed Fuzzy-PI controller is very effective in improving the fault ride through capability of overall wind farm system during fault conditions.

References

- [1] The Global Wind Energy Council (GWEC), Global wind report 2010, April 2011. [Online]. Available: <http://www.gwec.net>.
- [2] R. Doherty, E. Denny, and M. O'Malley, "System operation with a significant wind power penetration", IEEE Power Engineering. Summer Meeting, vol. 1, pp. 1002-1007, 6-10 Jun. 2004.
- [3] K.S. Salman and A.L.J. Teo, "Windmill modeling consideration and factors influencing the stability of a grid-connected wind power-based embedded generator," IEEE Trans. Power Syst. vol. 18, no. 2, pp. 793-802, May 2003.
- [4] Z. Litipu and K. Nagasaka, "Improve the reliability and environment of power system based on optimal allocation of WPG", IEEE. Power Systems Conf. Expo., vol. 1, pp. 524-532, 10-13 October. 2004.
- [5] N. Dizdarevic, M. Majstrovic, and S. Zutobradic, "Power quality in a distribution network after wind power plant connection", IEEE Power Syst. Conf. Expo., vol. 2, pp. 913-918, 10-13 October 2004.
- [6] Jauch C, Matevosyan J, Ackermann T, Bolik S., "International comparison of requirements for connection of wind turbines to power systems", Wind Energy, vol. 8, no. 3, pp. 295-306, July 2005.
- [7] Thomas Ackermann, Wind power in power system, UK: John Wiley & Sons, 2005, pp.53-65.
- [8] J. Tamura, T. Yamazaki, M. Ueno, Y. Matsumura, and S. Kimoto, "Transient stability simulation of power system including wind generator by PSCAD/EMTDC", IEEE Porto Power Tech, vol. 4, Paper no. EMT-108, 10-13 September 2001.
- [9] C.L. Souza et al, Power system transient stability analysis including synchronous and induction generator", IEEE

- Porto Power Tech Proceeding, Vol. 2, pp.6. 10-13 September 2001.
- [10] E. S. Abdin and W. Xu, "Control design and dynamic performance analysis of a wind turbine-induction generator unit", IEEE Trans. Energy Convers., vol. 15, no. 3, pp. 91-96, March 2000.
- [11] S. M. Muyeen, M. A. Mannan, M. H. Ali, R. Takahashi, T. Murata, and J. Tamura, "Stabilization of wind turbine generator system by STATCOM", IEEJ Trans. Power Energy, vol. 126, no. 10, pp.1073-1082, October 2006.
- [12] S. G. Bharathi Dasan, S. Ravichandran, R. P. Kamesh Kumudini Devi, "Steady-state analysis of Grid connected WECS using FACTS controller", International Conference on Emerging Trends in Electrical and Computer Technology (ICETECT), pp. 127-132. 23-24 March 2011.
- [13] L. Gyugyi: "Unified power flow control concept for flexible ac trans-mission system", Inst. Elect. Eng. C. vol. 139. no. 4, pp. 323-331, July 1992.
- [14] M.R.I.Sheikh, S.M. Muyeen, R. Takahashi, J.Tamura, "Smoothing Control of Wind Generator Output Fluctuations by PWM Voltage Source Converter and Chopper Controlled SMES", European Trans. Electrical Power, vol. 21, issue-1, pp. 680-697, January 2011.
- [15] S. M. Muyeen, R. Takahashi, T. Murata, J. Tamura, and M. H. Ali, "Transient stability analysis of permanent magnet variable speed synchronous wind generator", Int. Conf. Electrical Machines and Systems 2007, Seoul, Korea, pp. 288-293, 8-11 October 2007.
- [16] A. D. Hansen and G. Michalke, "Modelling and control of variable speed multi-pole permanent magnet synchronous generator wind turbine", Wind Energy, vol. 11, no. 5, pp. 537-554, 2008, 10.1002/we.278.
- [17] S. M. Muyeen, J. Tamura, and T. Murata, Stability augmentation of a grid connected wind farm, Green Energy and Technology, London, Springer-Verlag, 2009.
- [18] J. W. Dixon, J. M. Contardo, and L. A. Moran, "A Fuzzy controlled active front-end rectifier with current harmonic filtering characteristics and minimum sensing variable," IEEE Transaction on Power Electronics, vol. 14, no. 4, pp. 724-729, July 1999.
- [19] M. Rukonuzzaman, M. Nakaoka, "Fuzzy logic current controller for three-phase voltage source PWM-inverters", Industry Application Conference, Vol. 2, pp. 1163 - 1169, 8-12 October 2000.
- [20] Siegfried Heier, Grid integration of wind energy conversion systems, John Wiley & Sons Ltd 1998, pp. 34-36.
- [21] B. Farid O. Amar, "A Study of New Techniques of Controlled PWM Inverters", European Journal of Scientific Research, vol.32, no.1, pp. 77-87, 2009.